

ARTIFICIAL NEURAL NETWORKS IN FOREST BIOMASS ESTIMATION

Jalal Amini¹, Josaphat Tetuko Sri Sumantyo² Mahdi Falahati¹, and Reza Shams¹

¹ Department of Surveying engineering, Faculty of Engineering, University of Tehran, Tehran, Iran

E-mail: jamini@ut.ac.ir

² Centre for Environmental Remote sensing, Chiba University, Chiba, Japan

Email: jtetukoss@faculty.chiba-u.jp

ABSTRACT: In this paper, ALOS-AVNIR, PRISM, and JERS-1 images are used in a multilayer perceptron neural network (MLPNN) that relates them to forest variable measurements on the ground. The structure of this MLPNN is a three layers neural network that contains eight input neurons, 10 hidden neurons and five output neurons. It is shown that the biomass estimation accuracy is significantly improved when the MLPNN is used in comparison with Maximum Likelihood algorithm.

KEY WORDS: ALOS, MLPNN, SAR, biomass, neural network.

1. INTRODUCTION

Above ground biomass (AGB) is related to many important components, such as carbon cycles, soil nutrient allocations, fuel accumulation, and habitat environments in terrestrial ecosystems. The AGB governs the potential carbon emission that could be released to the atmosphere due to deforestation and change of regional AGB is associated with changes in climate and ecosystem. Different approaches, based on (1) field measurement (Brown et al. 1989, Brown and Iverson 1992, Schroeder et al. 1997, Houghton et al. 2001, Brown 2002), (2) remote sensing (Tiwari 1994, Roy and Ravan 1996, Tomppo et al. 2002, Foody et al. 2003, Zheng et al. 2004, Lu 2005), and (3) GIS (Brown and Gaston 1995) have been applied for AGB estimation. Traditional techniques based on field measurement are the most accurate ways for collecting biomass data. A sufficient number of field measurements is a prerequisite for developing AGB estimation models and for evaluating the AGB estimation results. However, these approaches are often time consuming, labour intensive, and difficult to implement, especially in remote areas; also, they cannot provide the spatial distribution of biomass in large areas. GIS-based methods using ancillary data are also difficult because of problems in obtaining good quality ancillary data, indirect relationships between AGB and ancillary data, and the comprehensive impacts of environmental conditions on AGB accumulation. Hence, GIS-based approaches have not applied extensively for AGB estimation. The advantages of remotely sensed data, such as in repetitively of data collection, a synoptic view, a digital format that allows fast processing of large quantities of data, and the high correlations between spectral bands and vegetation parameters, make it the

primary source for large area AGB estimation, especially in areas of difficult access. Therefore, remote sensing-based AGB estimation has increasingly attracted scientific interest.

This paper describes a method for estimating frost biomass based on both SAR image texture and multispectral optical image. We intend exploring the effect of neural networks in improving biomass estimation.

2. STUDY AREA AND DATA SETS

The study area for this project is the drainage basin of Shafarood in the north of Iran around the city Rezvanshahr (figure 1). It is located between $37^{\circ}24'N - 37^{\circ}40'N$ and $48^{\circ}46'E - 49^{\circ}11'E$. It is representative of the rugged mountainous landscape with various types of trees consist of: Maple, Alder, Conifer, Beech, Hornbeam, Azedarach and Acorn. Remote sensing data also consist of: AVNIR-2 and PRISM images from ALOS and a JERS-1 image. The JERS-1 image has a spatial resolution of approximately 13m and also, AVNIR-2 and PRISM images have the spatial resolutions of 10m and 2.5m respectively.

3. PREPROCESSING OF DATA SETS

SAR image consists of two components: backscatter coefficient, which contains information about the scene, and speckle fluctuations, which are produced by the imaging process. Both the radiometric and texture aspects are less efficient for area discrimination in the presence of speckle. Reducing the speckle would improve the discrimination among different land use types, and would make the usual per-pixel or textual classifiers more

efficient in radar images. Ideally, this supports that the filters reduce speckle without loss of information. In the case of homogeneous areas (e.g. agricultural areas), the filters should preserve the backscattering coefficient values (the radiometric information) and edges between the different areas. In addition for texture areas (e.g. forest), the filter should preserve the spatial variability (textual information).

Many adaptive filters that preserve the radiometric and texture information have been developed for speckle reduction. These filters are based on either the spatial or the frequency domain. Adaptive filters based upon the spatial domain are more widely used than frequency domain filters. The most frequently used adaptive filters include: Kuan, Gamma, Enhanced Lee, and Enhanced Frost filters (Lee 1980; Frost et al. 1982; Lopes et al. 1990; Kuan et al. 1987). These filters are applied on the JERS-1 image to find the filter that preserve the texture information for the study area. The ratio of the original intensity image to the filtered image enable us to determine the extent to which the reconstruction filter introduces radiometric distortion so that the reconstruction departs from the expected speckle statistics.

Suppose that the filters yield the true radar cross section (RCS), σ_j , at pixel j . The ratio of the pixel intensity in the JERS-1 image to the derived RCS, $r_j = I_j / \sigma_j$, should then correspond to speckle fluctuations along with a mean value of one. The mean and standard deviation (SD) can then be estimated over the ratio images. When the observed mean value differs significantly from one, it is an indication of radiometric distortion. If the reconstruction follows the original image too closely, the standard deviation would be expected to have a lower value than predicted. It would be larger than predicted if the reconstruction fails to follow genuine RCS variations. This provides a simple test that can be applied to any form of RCS reconstruction filters. The mean and standard deviation values of the ratio images are shown in table 2 for the JERS-1 image.

According to Table 1, the Gamma and Enhanced Lee filters have better results than others filters in this study. In this paper the Enhanced Lee filter with size of 5×5 was chosen after several tests.

Table 1. the mean and SD values of ratio images for the de-speckling filters

Filters	Frost	Kuan	Lee	Enhanced Frost	Enhanced Lee	Gamma
Mean	0.9449	0.9476	0.9545	0.9503	0.9656	0.9564
SD	0.0231	0.0252	0.0224	0.0293	0.0211	0.0211

After reduction the speckle noise, the texture of SAR image must be measured. Of the many describing texture methods, the grey-level co-occurrence matrix (GLCM) is the most common in remote sensing.

Nine texture measures are calculated from the GLCM for a moving window with size of 5×5 pixels that centered in pixel i, j of the de-speckled JERS-1 image. After the Gram-Schmidt process, just four texture measures: contrast, correlation, maximum probability and standard-deviation were selected as the optimum measures for this area.

The PRISM image is transformed in the universal transverse Mercator projection with a WGS84 datum based on the GPS measurements and is used as the base map. The GPS measurements are done with two GPSs that track along the roads of the study area. To place all data in a unified coordinate system, the AVNIR and JERS-1 image are registered to this map. Figure 1 is a red-green-blue (RGB) image overlay of PRISM, AVNIR, and JERS-1 images respectively of the study area. Red line indicates the path tracking by GPS.

The co-registered and geo-referenced data sets are used to extract digital numbers and texture feature vectors

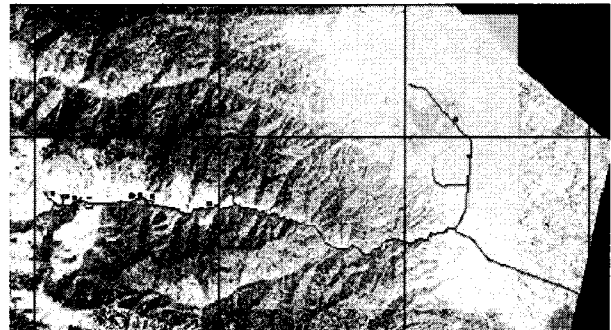


Figure 1. The RGB image overlay of PRISM, AVNIR, and JERS-1 images respectively. Red line indicates the GPS measurements

4. BIOMASS ESTIMATION

The co-registered and geo-referenced data sets are used to extract digital numbers (DN) and texture features from PRISM, AVNIR, and JERS-1 images respectively. The data are related to the forest biomass through a classification analysis. The correspondence between the remote sensing and ground data is made using PCI-Geomatica software, where the ground plot GPS locations are superimposed on the data set. For each of these points, a 5×5 window around the point is used and the average DN values of the PRISM and three channels of the AVNIR images with four texture values of the JERS-1 image are calculated. The values of these points (performed a vector for each point with eight elements) are used as training patterns.

The classification analysis is done with a multi layers perceptron neural network (MLPNN). A multi layers neural network is made up of sets of neurons assembled in a logical way and constituting several layers.

The network that is used in this study arrange in layers as following. The number of neurons in the output layer is taken to be equal to the number of classes desired for the classification. Here, the output layer of the neural network used to categorize the image in five classes should contain five neurons. The input layer has eight neurons corresponding to the number of attributes in the input vectors. After the determination of the input layer, the number of hidden layers required as well as the number of neurons in these layers still needs to be decided upon. An important result, established by the Russian mathematician Kolmogorov in the 1950s, states that any discriminate function can be derived by a three-layer feed-forward neural network (Duda et al. 2001). Increasing the number of hidden layers can then improve the accuracy of the classification, pick up some special requirements of the recognition procedure during the training or enable a practical implementation of the network. However, a network with more than one hidden layer is more prone to be poorly trained than one with only one hidden layer.

To summarize, the structure of multilayer neural network which was accordingly implemented is a 8-10-5 neural network (three layers: eight input neurons, ten hidden neurons and five output neurons) for classifying the data into five classes.

Training the neural network involves tuning all the synaptic weights so that the network learns to recognize given patterns or classes of samples sharing similar properties. The learning stage is critical for effective classification and the success of an approach by neural networks depends mainly on this phase.

The network is trained by using back-propagation rule (Paola and Schowengerdt, 1995).

The network is trained when all training patterns have been learnt. Once the network is trained, the weights of the network are applied on the data sets to classify into five classes: class1: Maple, class2: Alder, class3: Conifer, class4: Nursery and class5: None. Figure 2 shows the result after classification of the image with the MLPNN.

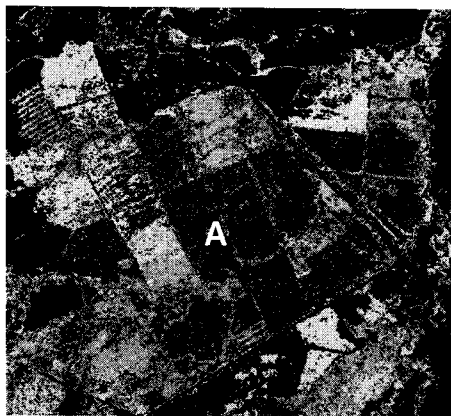


Figure 2. The classified image for site1 based on the MLPNN

Class 1: ■, Class 2: ■, Class 3: ■, Class 4: ■, Class 5: ■

Finally, we can estimate the biomass of the classes in the classified images. This was done for three classes in figure2 based on the allometric equation. Table 1 shows the estimated biomass for each class in figure 1.

Table 1 Estimated biomass using MLPNN classification for figure 2 by both optical and SAR data

	Conifer	Alder	Maple
Area (ha)	292.934	93.138	326.271
Mean height (m)	27.5	29	26.5
Mean DBH (cm)	40	40	35
# of tree (ha)	86	86	86
Mean biomass (kg/tree)	1434	1028	1509
Total biomass (tons/ha)	36115.4	28834.04	12091.39

4. CONCLUSION

In this paper, we demonstrated that a MLPNN is more successful for AGB estimation in forests. Textures in SAR images also played an important role in improving AGB estimation performance, especially for those sites with complicated forest stand structure. A combination of spectral responses and textures improved AGB estimation performance comparing pure spectral responses or textures. The complexity of forest stand structure is the main factor making the AGB estimation difficult.

5. REFERENCES

- BROWN, S., 2002, Measuring carbon in forests: current status and future challenges. *Environmental Pollution*, 116, pp. 363–372.
- BROWN, S. and GASTON, G., 1995, Use of forest inventories and geographic information systems to estimate biomass density of tropical forests: application to tropical Africa. *Environmental Monitoring and Assessment*, 38, pp. 157–168.
- BROWN, S., GILLESPIE, A.J.R. and LUGO, A.E., 1989, Biomass estimation methods for tropical forests with applications to forest inventory data. *Forest Science*, 35, pp. 881–902.
- BROWN, S. and IVERSON, L.R., 1992, Biomass estimation for tropical forests. *World Resource Review*, 4, pp. 366–384.
- DUDA, R.O., HART, P.E. and STORK, D.G., 2001, *Pattern Classification, 2nd edition* (New York: John Wiley and Sons).

FOODY, G.M., BOYD, D.S. and CUTLER, M.E.J., 2003, Predictive relations of tropical forest biomass from Landsat TM data and their transferability between regions. *Remote Sensing of Environment*, 85, pp. 463–474.

FROST, V. S., Stiles, J. A., Schanmugan, K. S., and Holzman, J. C., 1982, A model for radar images and its application to adaptive digital filtering of multiplicative noise. *IEEE Transactions on Pattern Analysis and Machine Intelligence*, 4, 157–166.

HOUGHTON, R.A., LAWRENCE, K.T., HACKLER, J.L. and BROWN, S., 2001, The spatial distribution of forest biomass in the Brazilian Amazon: a comparison of estimates. *Global Change Biology*, 7, pp. 731–746.

KUAN, D. T., Sawchuk, A. A., Strand, T. C., and Chavel, P., 1987, Adaptive restoration of images with speckle, *IEEE Transactions on Acoustics, Speech, and Signal Processing*, 35, 373–383.

LEE, J. S., 1980, Digital image enhancement and noise filtering by use of local statistics. *IEEE Transactions on Pattern Analysis and Machine Intelligence*, 2, 165–168.

LOPES, A., Touzi, R., Nezry, E., 1990, Adaptive speckle filters and scene heterogeneity. *IEEE Transactions on Geoscience and Remote Sensing*, Vol. 28, No. 6, pp. 1953–1962.

LU, D., 2005, Aboveground biomass estimation using Landsat TM data in the Brazilian Amazon Basin. *International Journal of Remote Sensing*, 26, pp. 2509–2525.

PAOLA J., and SCHOWENGERDT R.A., 1995, A review and analysis of back-propagation neural networks for classification of remotely-sensed multi-spectral imagery. *International journal of remote sensing*, Vol. 16, pp: 3033-3058.

ROY, P.S. and RAVAN, S.A., 1996, Biomass estimation using satellite remote sensing data—an investigation on possible approaches for natural forest. *Journal of Bioscience*, 21, pp. 535–561.

SCHROEDER, P., BROWN, S., MO, J., BIRDSEY, R. and CIESZEWSKI, C., 1997, Biomass estimation for temperate broadleaf forests of the US using inventory data. *Forest Science*, 43, pp. 424–434.

TIWARI, K.A., 1994, Mapping forest biomass through digital processing of IRS-1A data. *International Journal of Remote Sensing*, 15, pp. 1849–1866.

TOMPO, E., NILSSON, M., ROSENGREN, M., AALTO, P. and KENNEDY, P., 2002, Simultaneous use of Landsat-TM and IRS-1C WiFS data in estimating large area tree stem volume and aboveground biomass. *Remote Sensing of Environment*, 82, pp. 156–171.

ZHENG, D., RADEMACHER, J., CHEN, J., CROW, T., BRESEE, M., LE MOINE, J. and RYU, S., 2004, Estimating aboveground biomass using Landsat 7 ETM+ data across a managed landscape in northern Wisconsin, USA. *Remote Sensing of Environment*, 93, pp. 402–411.

6. Acknowledgement

Thanks UNIVERSITY OF TEHRAN VICE CHANCELLOR FOR RESEARCH supported the first author. Thanks the MRS Lab. in Centre for Environmental Remote Sensing, Chiba University, Japan.